Presented at IMAC 18, Feb 7-10, 2000, San Antonio, Texas.

IDENTIFYING DAMAGE SENSITIVE FEATURES USING NONLINEAR TIME-SERIES AND BISPECTRAL ANALYSIS

Debra George[1], Norman Hunter[2], Charles Farrar[3], Rebecca Deen[4]

[1]Undergraduate Research Assistant, University of Texas at El Paso
[2]Measuements Technology Group, MS C931, Los Alamos National Laboratory, Los Alamos, NM, 87545
[3]Engineering Analysis Group, MS P946, Los Alamos National Laboratory, Los Alamos, NM, 87545
[4]Undergraduate Research Assistant, University of Florida

ABSTRACT

The process of implementing a damage detection strategy for aerospace, civil, and mechanical engineering systems is called structural health monitoring*. Vibration-based damage detection is receiving considerable attention from the research community for such monitoring. Recent research has recognized that the process of vibration-based structural health monitoring is fundamentally one of statistical pattern recognition. This process is composed of four steps: 1.) Operational evaluation; 2.) Data acquisition and cleansing; 3.) Feature selection and data compression, and 4.) Statistical model development. This paper focuses on the development of damage sensitive features in systems exhibiting nonlinear response. Two features extraction methods are emphasize; nonlinear time-series analysis and bispectral analysis. These techniques are applied to data from a concrete column that was progressively damaged by quasi-static cyclic loading.*

1. INTRODUCTION

As our nation's infrastructure ages, the ability to monitor and accurately predict damage in structural systems becomes increasingly important. Many methods of detecting damage have been proposed. One of the approaches that has received considerable attention in the technical literature is vibration-based damage detection. The process of vibration-based damage detection is fundamentally one of statistical pattern recognition. Applying a statistical pattern recognition approach to this problem involves the following four steps: 1.) Operational evaluation; 2.) Data acquisition and cleansing; 3.) Feature selection and data compression, and 4.) Statistical model development, [1]. The discussion herein focuses on Step 3, feature selection for damage detection. Reference [2] summarizes many features that have been proposed for vibration-based damage detection. The majority of features described in this review are based on linear, time-invariant, modal analysis concepts. However, many damage scenarios cause the structure to respond in a nonlinear and non-stationary manner. Examples of such damage are the formation of cracks that subsequently open and close under normal operating conditions and the loosening of bolted joints.

The methods of feature extraction discussed in this study detect nonlinear behavior. Specifically they are non-linear Canonical Variate Analysis (CVA) and Bispectral Analysis. Data measured during vibration tests on a reinforced concrete column in an undamaged state and in progressively higher damaged states are analyzed.

2. STRUCTURAL MONITORING OF CONCRETE COLUMN

The data are from the UC-Irvine bridge column tests, which are described in detail in other IMAC papers [1,3]. Data consist of time histories from 40 accelerometers mounted on the column shown in Fig. 1.

Acceleration responses were measured during a series of cases, each with a greater degree of damage. Tests numbered 6 through 11 were from a shotcrete column (6 undamaged, 11 most damaged.) File designations ending in

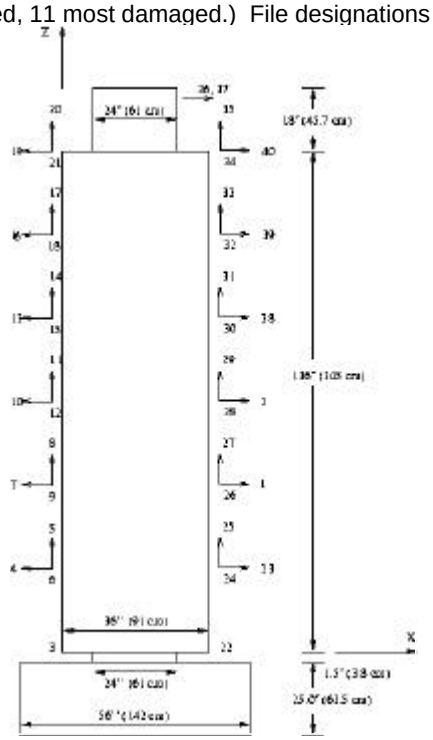

Fig. 1 Accelerometer locations

't' were from 8-s-long time series data sets consisting of 8192 data points. Files without a 't' are from 2-s-long data sets consisting of 2048 data points.

3. CVA PROCESSING

Local Canonical Variate Analysis (CVA) [4] models a nonlinear system using a series of local linear state space models. As implemented here, CVA is a time series technique. At any given time, future waveforms are modeled as a linear function of past waveforms. The process is quite similar to the traditional ARMA (Autoregressive Moving Average) model with the addition of a step that selects the most important waveforms from the past and future of the time series. The amplitudes of these critical waveforms form the "states" of the CVA model. The process is described in detail in reference [4].

The parameters of each linear model are determined from local regions of the measured time history data. A linear local state space model at the current time point is constructed using the waveforms that are similar to the reference waveform at current time. This approach is conceptually similar to the well-known process of representing the behavior of a nonlinear system by a Taylor series about an operating point. Local linear models are computed for each of a series of time points. The canonical variate analysis process [5] is employed to optimize each linear model. Estimated states are used to compute the temporal variation of resonant frequencies, damping values, and mode shapes. Future responses are predicted from the estimated states.

Non-linear CVA was used to model each test case of the concrete column. Twelve channels of accelerometer data were processed; four channels in each direction (x, y, and z.) For the 8192 pt time series 2500 training points were used, to construct the CVA model. For the 2048 point time series 1400 training points were used for model construction. An optimal model was obtained using ten states. Eight Time series values from each of the twelve locations formed the past and future time series from which the model was constructed. The number of lags was chosen to provide about a cycle of the lowest frequency of interest in the data, while the number of states was chosen by minimizing the time series prediction error. Twelve locations on the concrete column provided a reasonable compromise between using all the column locations (more processing time) and a few locations (poor model spatial resolution).

4. DAMAGE SENSITIVE FEATURE DETECTION USING CVA

Nonlinear CVA estimates system poles, from which frequency and damping values are derived, along with time varying spatial mode shapes. These features are estimated as functions of the local time series so a set of poles and mode shapes are obtained for each local linear model. For a globally linear system a single set of poles and mode shapes describe the system behavior at any time. For a nonlinear system the pole locations and the mode shapes change systematically with time.

Several types of changes in the poles are related to the damage. Figure 2 shows the pole locations for the undamaged case and for five cases of successively increasing damaged. Note that for these Z plane poles, the pole angle with respect to the x axis is proportional to frequency, with 180 degrees corresponding to the Nyquist frequency. Pole distance from the origin is related to damping, with greater damping corresponding to a smaller radius. Additional poles appear at some of the damage levels. For example, damage levels 3, 4, and 5 all show 3 poles, while level 2 shows two poles. The undamaged case, Level 1, shows a single pole in the range of interest. See Fig. 2, below.

All of the poles show evidence of nonlinear or noisy behavior, as indicated by the scatter in the pole locations. This scatter corresponds to local variations in frequency and damping. The arrows indicate the pole set in question. Other poles occur at frequencies (angles) above and below the indicated set and correspond to other column modes. Note that the damage causes decreased in frequency followed by an increased as shown by the decreasing and then increasing angle. Damping increases (pole radius decreases) at damage levels 1-3. Damping then decreases at damage levels 4 and 5.

In general, considering all of the pole sets, the scatter for certain poles is greater in the damaged cases but this result doesn't occur consistently for all poles and is hard to evaluate because damaged cases usually have extra poles. It is clear that the column has a number of modes, and that

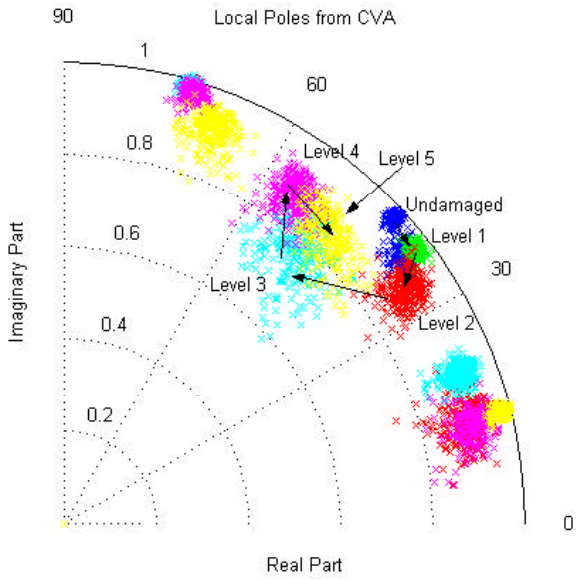

Fig. 2 Local (successive) Poles from Nonlinear CVA using 5 Hz. High pass filter, 8 lags, 10 states at successively greater levels of damage to the shotcrete column.

damage introduces modes that did not exist in the undamaged case. To derive a single indicator of damage suitable for statistical pattern recognition, two methods were investigated; Frequency Analysis and Mode Shape Analysis. Both are described below.

FREQUENCY ANALYSIS:

Frequencies, damping values and mode shapes were obtained from the Nonlinear CVA State Model. The poles were found through cluster analysis.

The frequencies and damping values were analyzed and weighted with less emphasis on frequency and damping values with more scatter. Damping values, ξ, were found from Equation (1), where da is the pole radius from Figure 2, f_s is the sampling frequency, and f_n is the natural frequency corresponding to the pole location

$$\xi = \frac{\ln(da) f_s}{4\pi f_n} \qquad (1)$$

A sum of the weighted damping values is plotted in Figure 3, where the results of several different local CVA models are shown. The models differ in the number of time values forming the past and future of the time series (8 or 20, corresponding to the 8 or 20 lag cases), and in the filtering used on the time series data prior to construction of the CVA models (5 Hz. High pass, or no pre-filtering, 0 Hz.). The 20 lag case detected a low frequency pole in a few cases, which increased the effective sum of damping values as indicated in Figure 3. Excluding the very low frequency poles, damage corresponded to any damping sum greater than twice the initial weighted damping level. This result holds true for all damage levels above 1 Δy (Test 7).

Note the initial increase in weighted damping values with damage levels 1 (test 7) and 2 (test 8), followed by a decrease in weighted damping values for damage levels 4 (test 9) and 5 (test 10).

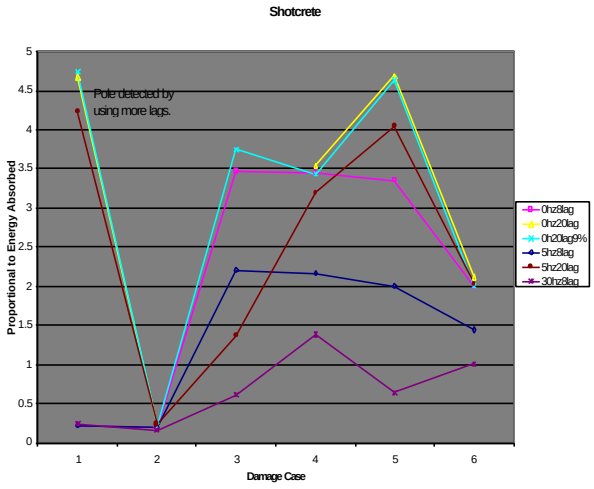

Fig. 3 Weighted Damping Sum for Several Local CVA Models.

MODE SHAPE ANALYSIS:

Mode shapes were examined to see if damage corresponded to change in the mode shapes. Local Linear CVA provides estimates both the mode shapes and their variation as a function of the local time history. There were obvious differences in mode shapes when the column was damaged, but those differences did not follow a consistent trend, in the sense that more damage led to more mode shape change in a given direction. Local scatter in successive mode shapes (as a function of time), estimated from the local linear CVA, likewise didn't follow obvious trends based on the damage level.

Because trends seemed inconsistent, or at least difficult to interpret, mean values from the undamaged case were used as baseline shapes, and deviations from these examined as a function of damage. X and Y, and Z directions were examined separately.

Each case was processed as follows: The mean mode value was found for each mode and spacial location. The undamaged mean modal values were subtracted from the damaged mean mode values. The absolute values of these differences were summed across all locations and modes, yielding a single value that quantified the overall change in mode shape as a function of damage. Table 1 lists these values as a function of damage level and direction. For undamaged, or reference case, the modal values were summed directly. Because the baseline case is a reference case, parameter values show changes with respect to the reference. In nearly every instance, the damaged case comes out with a higher parameter value than the baseline (undamaged) value. This method works particularly well for the 5 Hz, 8 lags case. This analysis was performed on the 8196 pt and 2048 pt time series data. The parameter increases with damage, but not uniformly, since, for example, in the Y direction, the 4 Δy case has a lower value (2.08) than does the 1.5 ΔY case (2.60). Because the "modal damage parameter" didn't increase uniformly with damage level, further investigations were made.

MODE PARAMETER VALIDATION

The purpose of damage detection is to quantify the probability that damage exists, thus defining the probability of false positives and false negatives. A false positive occurs when damage is predicted, and none in fact exists. Conversely, a false negative occurs when no damage is predicted when in fact damage exists. In order to simulate a large set of test cases, each individual mode shape (damaged and undamaged) was used as a test case. A difference from the undamaged modal value was then available for each mode. A probability density function of P(m) for each damage level was calculated using Equation 2. This probability density was calculated over each mode shape difference m. The probabilities in Table 2 are thus functions of the modal difference m, the numerator of Equation 2.

$$p(m) = \frac{\sum_{DOF} abs(DSV - UDSV)}{\sum_{DOF} abs(UDSV)} \qquad (2)$$

$$0 \le m \le no.of\ mod\ es$$

Where DSV is the damaged mode shape value and UDSV is the undamaged mode shape value.

Table 1

Comparison of Mode Parameters

	8196 Pt Data		
	X Parameter	Y Parameter	Z Parameter
Undamaged	(1.00)	(1.00)	(1.00)
1 Δy	2.11	2.27	1.61
1.5 Δy	2.60	2.24	2.28
2.5 Δy	2.08	2.36	2.09
4 Δy	2.81	2.17	2.19
7 Δy	2.43	2.24	2.35
	2048 Pt. Data		
	X Parameter	Y Parameter	Z Parameter
Undamaged	1.00	1.00	1.00
1 Δy	N/A	N/A	N/A
1.5 Δy	2.3	2.36	2.38
2.5 Δy	2.8	2.49	1.32
4 Δy	2.4	2.14	3.33
7 Δy	1.5	2.31	3.31

Intersections of the undamaged and damaged areas are integrated and squared to yield the probabilities of false positives in Table 2. The probability density functions are shown in Fig. 4.

Table 2
Probability of False Positive Based On Mode Shape Changes

	5hz8lag\ Test6t-11t	5hz8lag\ Test6-11
Undamaged	-	-
1 Δy	28.98%	-
1.5 Δy	1.88%	17.51%
2.5 Δy	11.82%	8.23%
4 Δy	3.67%	1.91%
7 Δy	18.33%	2.55%

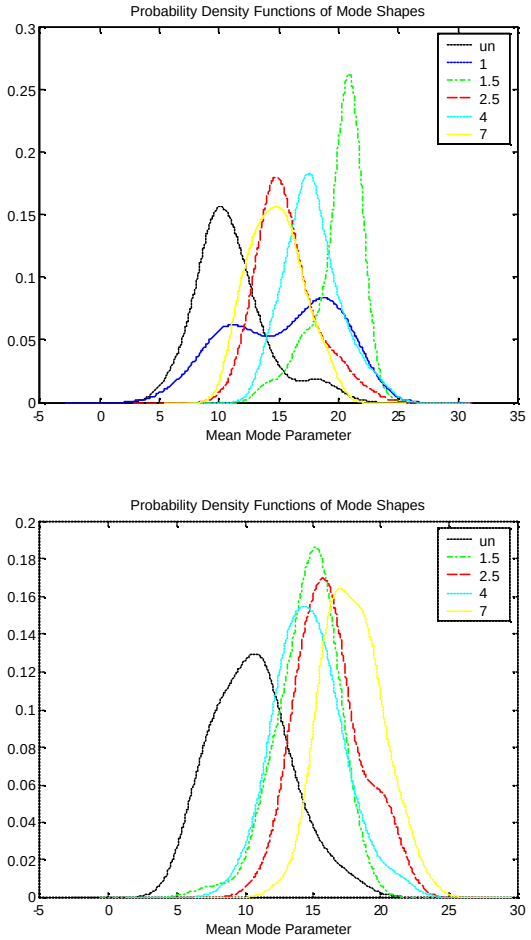

Fig 4. Probability Density Functions of Mode shapes from Shotcrete column, 5 Hz, 8 lag CVA results. Above: from 8192 point time series test data, Below: from 2048 point time series.

BISPECTRAL ANALYSIS

The power spectrum is the frequency domain decomposition of signal power. When this concept is extended to higher orders, the result is a polyspectrum. The third-order polyspectrum is the bispectrum. The bispectrum is defined as the frequency decomposition of the skewness, or third-order covariance function, of a signal. The bispectrum provides information regarding such signal features as phase coherence, which are absent in the second-order power spectrum. An important use of the bispectrum is the detection of nonlinearities. Because of its sensitivity to nonlinearities, it is believed that the bispectrum has practical uses in the area of structural health monitoring and damage detection. The bispectrum has been shown to be an indicator of fatigue cracks in cantilever beams [6] and has been applied to damage detection in rotating machinery [7].

For a discrete time series, the discrete bispectrum is defined as the double Fourier transform of the third order covariance function expressed as Equation (3) in the following ways:

$$B(f_1,f_2)=\sum_{k=-\infty}^{\infty}\sum_{l=-\infty}^{\infty}c_3(k,l)e^{-if_1k-if_2l}$$
$$=DFT^2[c_3(\tau_1,\tau_2)] \quad (3)$$
$$=E[X(f_1)X(f_2)X^*(f_1+f_2)]$$

where E denotes the expectation operator, * denotes complex conjugate, X(f) is the discrete Fourier transform, and the third-order covariance function, $c_3(k,l)$, is:

$$c_3(k,l)=E[x(t)x(t+k)x(t+l)]. \quad (4)$$

The bispectrum is a function of two different frequencies f_k and f_l. Only those bifrequencies (f_k,f_l) that fall within the following domain need be computed:

$$f_l \le f_k,\ 2f_k+f_l \le f_s$$

where f_s is the sampling frequency. All bifrequencies outside of this domain are redundant because of the symmetric properties of the bispectrum. A peak in the bispectrum at the bifrequency (f_k, f_l) indicates a coupling between the three frequencies f_k, f_l and $f_k + f_l$ and their corresponding phases ϕ_k, ϕ_l and ϕ_{k+l}. This frequency and phase coupling is the result of a quadratic type of nonlinearity in the process generating the signal.

In practice, a normalization of the bispectrum is commonly used. The normalized bispectrum is referred to as the bicoherence, $b^2(f_1,f_2)$, and is defined as:

$$b^2(f_1,f_2)=\frac{|B(f_1,f_2)|^2}{E[|X(f_1)X(f_2)|^2]E[|X(f_1+f_2)|^2]} \quad (5)$$

The bicoherence measures the percentage of power at frequency f_1+f_2 caused by signal coupling of components at f_1 and f_2. The bicoherence removes the dependency on amplitude, and takes on an amplitude value between 0 and 1. A Value of one indicates that all the energy at f_1+f_2 is from the coupling of components at f_1 and f_2. Therefore, this function can be used to detect the presence of harmonics.

The bicoherence function was used to analyze data from the shotcrete column. A code developed by Norman Hunter at Los Alamos National Laboratory, bicoc1, was used to calculate the bicoherence function. This code was applied to time histories measured at accelerometer 1 (see Fig. 1) when the column was in its undamaged state (Test 6), after it had been cycled to the first yield level (Test 7) and after it had been cycled to 2.5 times the first yield. (Test 9). For these calculations the 8192 pt time series were divide into 128 pt segments. A Hanning window was applied to each segment.

Figure 5 shows the bicoherence generated from the undamaged data. Most values lie below 0.05 and were verified to be the result of noise in the measurements and bicoherence calculations. For an undamaged linear system no frequency coupling is expected. When applied to test 7 and test 9 the bicoherence links a sum of frequencies, each near 210 Hz, to response at about 420 Hz. This result is clearly displayed in Figures 6 through 9.

Examination of the Power spectrum from accelerometer location 1, Tests 6, 7 and 9, shows peaks at 420 Hz as well as at 210 Hz (Figure 10). However, this plot gives no indication of the coupling between these frequencies that is evident in the bispectral plots.

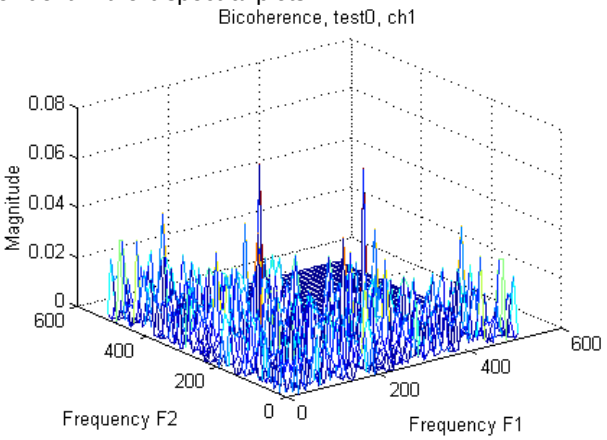

Fig. 5 Bicoherence function obtained from accelerometer 1 data measured on the undamaged column.

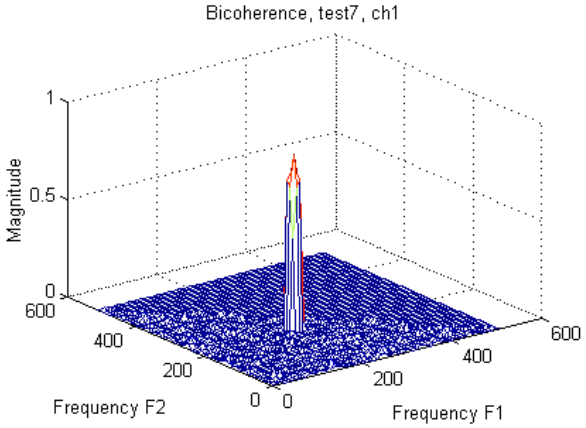

Fig. 6 Bicoherence function obtained from accelerometer 1 data after the shotcrete column had been cycled to the first yield level (Test 7).

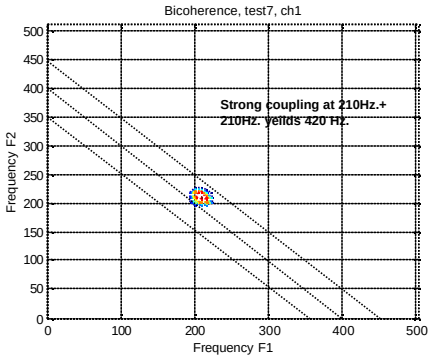

Fig. 7 A projection of the bicoherence function shown in Fig. B onto the F_1-F_2 plane.

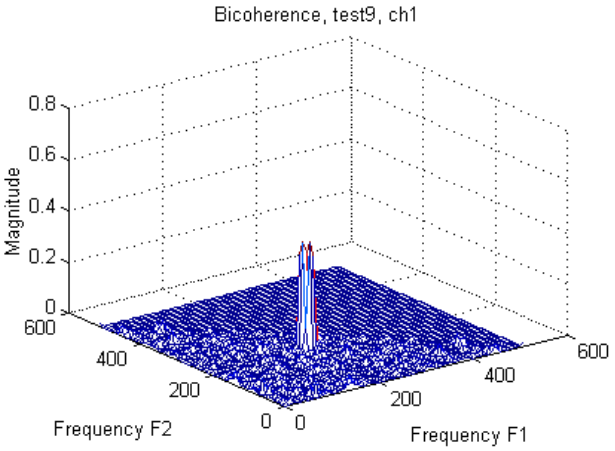

Fig. 8 Bicoherence function obtained from accelerometer 1 data after the shotcrete column had been cycled to a peak displacement of 2.5 times the first yield displacement (Test 9).

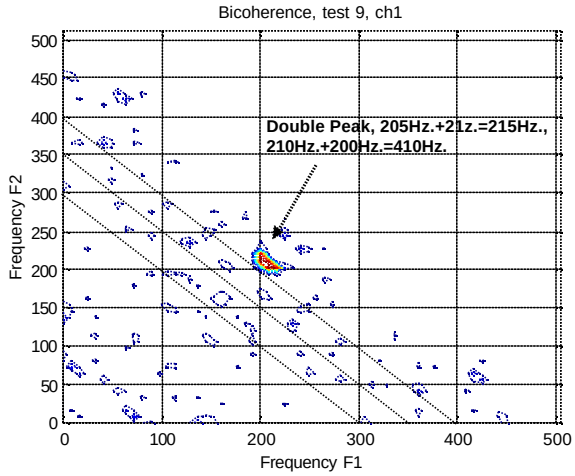

Fig. 9 A projection of the bicoherence function shown in Fig. D onto the F_1-F_2 plane.

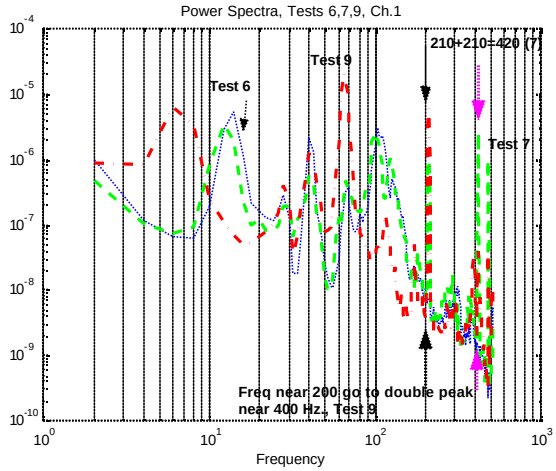

Fig. 10 Power Spectrum, accelerometer 1, Tests 6,7, and 9.

SUMMARY:

The focus of this paper has been on identifying damage sensitive features that capture nonlinear response characteristics of a structure. Canonical Variate Analysis and Bispectrum Analysis are two feature extraction procedures investigated in this study. Canonical Variate Analysis was used to identify temporal variations in the system state that are indicative of nonlinear behavior. The bispectrum analysis was used to identify coupling between measured response frequency components and is particularly sensitive to quadratic system nonlinearities. These feature extraction techniques were applied to acceleration data measured on a concrete column in its undamaged state and after various levels of damage had been applied through quasi-static cyclic loading.

Potential damage sensitive features derived from non-linear CVA include pole location, pole deviation, frequency and/or damping changes, and mode shape changes. For the system studied, scatter in the pole locations and mode shapes were less consistent indicators of damage as compared to shifts in the mean pole location, increase in the mean damping, and changes in the mode shapes. Although it is assumed that some damaged systems will show increases in nonlinear behavior with damage, this result was not observed in the CVA results for these columns. The authors' speculation for why this assumed trend in the features did not occur is discussed below.

The bicoherence showed significant changes between the data from the damaged column and data from the undamaged column. There is strong indication of coupling between the response measured at 210 Hz and the response measured at 420 Hz. This coupling is seen in various tests after the initial rebar yield. Although these same frequencies appear as peaks in the conventional power spectra, these spectra do not provide any indication of the coupling between response at these frequencies.

It is interesting to note that virtually every damage indicator shows a near immediate increase at the onset of damage, followed by a sort of "saturation" as the indicator changes much less at higher damage levels. At first, the authors expected to see increasing indications of damage at the higher levels of damage. However, when the structure reaches the first yield level (Test 7), strain compatibility requires the concrete to have cracked at this point. The permanent deformation is smallest at this first damage level and, hence, allows the greatest potential for the cracks to open and close during the subsequent dynamic excitation. As larger deformations are applied to the structure (Tests 8 – 11), the rebar progressively yields with more permanent deformation after the cyclic tests are complete. This permanent deformation tends to hold the cracks open and the low-level dynamic excitation, which was kept near constant amplitude during each test, does not excite the nonlinear response associated with the cracks opening and closing. At these higher damage levels the structure tends to respond as a reduced stiffness system, with different dynamic properties than those exhibited by the undamaged system or the system after it had reached initial rebar yield.

The tests analyzed in this study were performed in a laboratory and, therefore, had minimal operational and environmental variability associated with them. However, for field application one will have to separate variability in the identified features caused by damage from variability caused by changing environmental and operating conditions. To perform such distinctions, one will have to apply some form of statistical pattern recognition to features, hopefully of low dimension, derived from the CVA or bispectral analysis. The authors are currently working on such statistical procedures as well as methods to reduce the results of these feature extraction methods to low-dimension, damage-sensitive features vectors.

Acknowledgements

Portion of the funding for this work has come from a cooperative research and development agreement with Kinemetrics Corporation, Pasadena California. The civilian application of this CRADA is aimed at developing structural health monitoring systems for civil engineering infrastructure. A portion of the funding for this research was provided by the Department of Energy's Enhanced Surveillance Program. Vibration tests on the columns were conducted jointly with Prof. Gerry Pardoen at the University of California, Irvine using Los Alamos National Laboratory's University of California Interaction Funds. CALTRANS provided the primary funds for construction and cyclic testing of the columns.

REFERENCES

1. Farrar, C. R., Doebling, S. W., and Nix, D. A. Damage identification with linear discriminant operators. 1999. Proceedings of the 17th International Modal Analysis Conference.

2. Doebling, S. W., Farrar, C. R., Prime, M. B., and Sheviz, D. W. Damage identification and health monitoring of structural and mechanical systems form changes in their vibration characteristics: a literature review. LA-13070-MS. 1996. Los Alamos National Laboratory.

3. Sohn, H, Fugate, M. and Farrar, C. Statistical Process Control Applied to Vibration-Based Damage. Detection, 2000. Proceedings of the 18th International Modal Analysis Conference.

4. Hunter, N. F. "Bilinear system characterization from nonlinear time series analysis". 1999. Proceedings of the 17th International Modal Analysis Conference.

5. Larimore, W. E. System identification, reduced order filtering, and modeling via. canonical variate analysis. Rao, H. S. and Dorato, P. 445-451. 1983. Proceedings of the 1983 American Control Conference.

6. Rivola,A. and P.R.White. 1998. Bispectal Analysis of the Bilinear Oscillator with Application to the Detection of Fatique Cracks. Journal of Sound and Vibration 216: 889-910.

7. C. J. Li, J. Ma, B. Hwang, and G.W. Nickerson, "Pattern Recognition Based Bicoherence Analysis of Vibrations for Bearing Condition Monitoring", *in Sensors, Controls, and Quality Issues in Manufacturing*, American Society of Mechanical Engineers (1991), pp.1-11.